BJ www.biochemj.org

BJ Cell

Biochem. J. (2009) **424**, 367–374 (Printed in Great Britain) doi:10.1042/BJ20090576

online data

Leishmania donovani Ran-GTPase interacts at the nuclear rim with linker histone H1

Despina SMIRLIS*[1], Haralabia BOLETI*†, Maria GAITANOU‡, Manuel SOTO§ and Ketty SOTERIADOU*

*Laboratory of Molecular Parasitology, Department of Microbiology, Hellenic Pasteur Institute, 127 Bas. Sofias Ave., 11521 Athens, Greece, †Light Microscopy Unit, Hellenic Pasteur Institute, 127 Bas. Sofias Ave., 11521 Athens, Greece, ‡Laboratory of Cellular and Molecular Neurobiology, Department of Biochemistry, Hellenic Pasteur Institute, 127 Bas. Sofias Ave., 11521 Athens, Greece, and §Centro de Biología Molecular Severo Ochoa (CSIC-UAM), Departamento de Biología Molecular, Universidad Autónoma de Madrid, 28049 Madrid, Spain

Ran-GTPase regulates multiple cellular processes such as nucleocytoplasmic transport, mitotic spindle assembly, nuclear envelope assembly, cell-cycle progression and the mitotic checkpoint. The leishmanial Ran protein, in contrast with its mammalian counterpart which is predominately nucleoplasmic, is localized at the nuclear rim. The aim of the present study was to characterize the *Ld*Ran (*Leishmania donovani* Ran) orthologue with an emphasis on the Ran–histone association. *Ld*Ran was found to be developmentally regulated, expressed 3-fold less in the amastigote stage. *Ld*Ran overexpression caused a growth defect linked to a delayed S-phase progression in promastigotes as for its mammalian counterpart. We report for the first time that Ran interacts with a linker histone, histone H1, *in vitro* and that the two proteins co-localize at the parasite nuclear rim. Interaction of Ran with core histones H3 and H4, creating in metazoans a chromosomal Ran-GTP gradient important for mitotic spindle assembly, is speculative in *Leishmania* spp., not only because this parasite undergoes a closed mitosis, but also because the main localization of *Ld*Ran is different from that of core histone H3. Interaction of Ran with the leishmanial linker histone H1 (LeishH1) suggests that this association maybe involved in modulation of pathways other than those documented for the metazoan Ran–core histone association.

Key words: cell cycle, chromosomal gradient, guanine-nucleotide-exchange factor (GEF), *Leishmania*, linker histone H1, Ran-GTPase.

INTRODUCTION

Ran-GTPase, or Ran, belongs to the Ras superfamily of monomeric G-proteins that switches between a GDP- and a GTP-bound form [1]. The transition from Ran-GDP to Ran-GTP occurs only by nucleotide exchange. The nucleotide-exchange factor RCC1 (regulator of chromosome condensation 1) catalyses this reaction and results in efficient generation of nuclear Ran-GTP [2]. The conversion of Ran-GTP into Ran-GDP is catalysed in the cytosol by Ran-GAP1, which activates Ran's intrinsic GTPase activity [3]. Ran is involved in multiple cellular processes such as modulation of nucleocytoplasmic transport of macromolecules across the nuclear envelope [4], mitotic spindle assembly [5], post-mitotic nuclear envelope assembly [6], cell-cycle progression [7] and the mitotic checkpoint [8].

The predominant localization of Ran in most eukaryotic cells is in the nucleoplasm, where it is found mostly in the GTP-bound form [7]. The Ran-GTP gradient across the interphase nuclear envelope and on the condensed mitotic chromosomes is essential for many cellular processes, including nucleocytoplasmic transport and spindle assembly [9]. The mammalian Ran is known to interact in the nucleoplasm with chromatin. This interaction occurs via two distinct mechanisms. One mechanism is the interaction of Ran with its nucleotide-exchange factor RCC1 which in turn interacts with histones H2A and H2B [10] and the other via a direct binding of Ran to histone H3 and histone H4 [11]. The Ran–RCC1 binary complex binds stably to chromatin and ensures that RCC1 couples its GEF (guanine-nucleotide-exchange factor) activity to chromosome binding [12]. Via these core histone–Ran and core histone–Ran–RCC1 interactions, at least in animal cells, Ran-GTP appears to form during mitosis a gradient with the highest concentration on the condensed chromosomes that tapers off towards the periphery of the cell [12]. Experiments in *Xenopus* egg extracts suggest further that a high Ran-GTP concentration near the chromosomes stimulates microtubule nucleation, whereas microtubule stabilization is favoured by the lower concentration of Ran-GTP found further away from the chromosomes [13]. These differential effects of Ran-GTP on microtubules could be critical for spindle assembly. Taken together, these findings indicate that the mitotic Ran-GTP chromosomal concentration gradient is important to navigate spindle assembly towards the condensed RCC1-rich chromosomes in animal cells.

The Ran-GTP chromosomal gradient is not so evident in systems where Ran is not predominantly nucleoplasmic. Only a few examples of non-nucleoplasmic localization of Ran are known to date. One such example is the localization of the Ran2 protein of *Arabidopsis*, a plant orthologue of Ran localized in the nuclear envelope/rim and in perinuclear structures [14]. Another example is *Toxoplasma gondii*'s Ran orthologue, which was detected throughout the cell [15]. Additionally the trypanosomatid *Lmj*Ran (*Leishmania major* Ran) fused to GFP (green fluorescent protein) was recently found to decorate a nuclear envelope 'collar' and to be closely associated with nuclear pore complexes [16].

Leishmania is a protozoan parasite, a member of the Trypanosomatidae family, which is responsible for a spectrum of diseases in humans. Depending on the *Leishmania* species and on the immunological response of the host, the disease

Abbreviations used: Ab, antibody; CAS, cellular apoptosis susceptibility; GFP, green fluorescent protein; GST, glutathione transferase; HU, hydroxyurea; INO1, *myo*-inositol-1-phosphate synthase; *Ld*Ran, *Leishmania donovani* Ran; LeishH, leishmanial histone; *Lin*INO1, *Leishmania infantum* INO1; *Lmj*Ran, *Leishmania major* Ran; mAb, monoclonal antibody; Ni-NTA, Ni^{2+}-nitrilotriacetate; NTF2, nuclear factor 2; ORF, open reading frame; pAb, polyclonal antibody; PI, propidium iodide; RCC1, regulator of chromosome condensation 1.

[1] To whom correspondence should be addressed (email penny@pasteur.gr).

ranges from self-healing skin lesions to life-threatening visceral leishmaniasis, causing extensive morbidity and mortality [17]. Worldwide, 14 million people are infected with *Leishmania*, with an estimated yearly incidence of 1.5–2 million new cases [17]. *Leishmania* is transmitted by the blood-sucking phlebotomine sandfly. During its life cycle, the parasite exists in two forms: as an extracellular flagellated promastigote in the insect vector, and in the non-motile amastigote form in the acidic phagolysosome of the macrophage in the mammalian host [18]. Recent advances in parasite differentiation and survival strategies within the macrophages have facilitated the understanding of key aspects of *Leishmania* pathogenesis, although many more remain unknown (reviewed in [19]).

The fundamental processes of cell biology mediated by Ran are expected to play a crucial role in survival and growth strategies of the Trypanosomatid parasites. A Ran orthologue in *Trypanosoma brucei*, rtb2 [20], has been shown to be an essential gene for parasite survival [16]. The *L. major* orthologue was identified recently and was shown to co-localize at the nuclear membrane with the homologue of nucleoporin Sec13 [16]. Several potential partners of *Lmj*Ran have been identified by BLAST search [NTF2 (nuclear factor 2), CAS (cellular apoptosis susceptibility), RanBP1 (Ran-binding protein 1)], and their localization matches the nuclear envelope localization of *Lmj*Ran [16].

The present paper describes the investigation of an interaction of *Ld*Ran (*Leishmania donovani* Ran) orthologue with the leishmanial histones H1, H2B and H3 (LeishH1, LeishH2B and LeishH3 respectively). *Ld*Ran was found to interact specifically with LeishH1 and co-localize with this histone at the nuclear rim. This is the first evidence of an interaction of a Ran protein with a linker histone, opening the field to a more in-depth investigation on the purpose of this interaction to the parasite's cell biology.

EXPERIMENTAL

Plasmids

The gene encoding *Ld*Ran (GenBank® accession number EU426549) was amplified by PCR, from genomic *L. donovani* (MHOM/ET/0000/HUSSEN) DNA. The forward and reverse primers used were 5′-TTTTGGAATTCTATGCAACAGGCACC-CTCG-3′ and 5′-ATGGGCGATGACGAGGGACTCGAGGCCG-3′ respectively, based on the *Leishmania infantum* DNA sequence. The PCR product was cloned in the EcoRI and XhoI site of the pTriex1.1 (Novagen), in-frame with the C-terminal His_6 tag to generate the pTriex-*Ld*Ran plasmid.

For the generation of a leishmanial *Ld*Ran expression plasmid, the *Ld*Ran-encoding DNA was amplified from genomic *L. donovani* (MHOM/ET/0000/HUSSEN) DNA by using as forward and reverse primers 5′-GCACGGATCCGTACACCATGCAAC-AGGCACC-3′ and 5′-GACACTCGAGGGGTCTCACTCGTCA-TC-3′ respectively. The PCR product was then digested with BamHI and XhoI and inserted in the BglII and XhoI site of the LEXSY-SAT vector, to generate the *Ld*Ran-SAT plasmid.

Murine Rab1a (GenBank® accession number AF226873) cDNA was amplified by RT (reverse transcription)–PCR using the forward and reverse primers, 5′-CGCGGATCCATGTCCAGCA-TGAATCCCG-3′ and 5′-ATAAGAATGCGGCCGCTTAGCAG-CAGCC-3′ respectively. The amplified product was cloned in the BamHI and NotI restriction sites of pGEX4T1 plasmid as a fusion protein with GST (glutathione transferase).

The LeishH1 gene was cloned in pGEX-4T1 as described previously [21]. The *INO1* (*myo*-inositol-1-phosphate synthase) gene was cloned in the pTriex1.1 plasmid as described previously [22].

Cell culture and transfection

L. donovani (MHOM/ET/0000/HUSSEN) promastigotes were cultured in Medium 199 containing 10 % (v/v) HIFBS (heat-inactivated fetal bovine serum) at 26 °C as described previously [21]. *L. donovani* parasites were transfected with the *Leishmania* SAT expression plasmid (supercoiled, transfected as episomes), *Ld*Ran-SAT, as described previously [21]. For selection of transgenic parasites, 100 μg/ml noursethricin (Jena Bioscience) was used. To assess the growth of these parasites, parasites were immobilized by the addition of 30 μl of 3.7 % (w/v) formaldehyde in 1 ml of PBS, and counted in a Malassez haemocytometer.

Axenic *L. donovani* amastigotes were generated as described previously [21].

SDS/PAGE and immunoblotting

SDS/PAGE was performed using the method of Laemmli [23]. For immunoblotting, proteins were transferred on to a nitrocellulose filter (Hybond C, GE Healthcare) and immunoblotting was performed as described previously with the use of 3,3′-diaminobenzidine as a chromometric substrate [24] or by ECL® Plus (enhanced chemiluminescence) (GE Healthcare) according to the manufacturer's instructions. For the quantification of immunoblot bands, AlphaImager software (Alpha Innotech) was used.

Production of recombinant proteins and generation of antibodies

Recombinant *Ld*Ran and *Lin*INO1 (*L. infantum* INO1) were generated as C-terminal His_6-tagged proteins in the *Escherichia coli* strain BL21 pLysS, as described previously [21] and the recombinant proteins were purified on a Ni-NTA (Ni^{2+}-nitrilotriacetate) matrix under denaturing conditions according to the manufacturer's instructions (Qiagen).

Loads of 300 μg (*Ld*Ran and INO1) and 30 μg (LeishH2B and LeishH3 [25] and *Ld*Ran) of recombinant proteins were used per injection for the immunization of two New Zealand white rabbits and two Balb/c mice respectively for each protein, as described previously [21]. All procedures involving animals were conducted in accordance with the European Guidelines, approved by the ethical committee of the Hellenic Parleur Institute. Affinity-purified Abs (antibodies) (anti-*Ld*Ran, anti-LeishH1, anti-LeishH2B and anti-LeishH3) were isolated by low-pH elution from nitrocellulose strips with purified *Ld*Ran, LeishH1, LeishH2B and LeishH3 respectively, as described previously [21]. A second step of affinity-purification of the anti-*Ld*Ran Ab, was followed to ensure its specificity.

Immunofluorescence

L. donovani promastigotes ($3–5 \times 10^6$/ml) were washed once with PBS and then fixed for 20 min at room temperature (25 °C) with PBS containing 2 % (w/v) paraformaldehyde or with ice-cold methanol for 5 min. The parasite cells were then permeabilized and blocked by incubation for 1 h at room temperature with blocking buffer (0.3 % BSA and 0.1 % Triton X-100 in PBS) and were subsequently stained with the affinity-purified anti-*Ld*Ran Ab (0.2 μg/ml) diluted in blocking buffer. For co-localization studies, affinity-purified rabbit anti-LeishH1 [21], mouse anti-LeishH2B, anti-LeishH3 and anti-*Ld*Ran pAbs (polyclonal Abs) were used at concentrations of 2–10 μg/ml. The commercially available mAb (monoclonal Ab) specific for nuclear pore complex proteins that recognizes the conserved

FXFG repeats in nucleoporins (Abcam) was used at a final concentration of 10 μg/ml. Incubation with the primary Abs, was performed overnight in a humid chamber at 4 °C. After extensive washing, the appropriate secondary Abs were added, Alexa Fluor® 546- and Alexa Fluor® 488-conjugated anti-rabbit and anti-mouse (Molecular Probes), at a final concentration of 2 μg/ml in blocking buffer, for 2 h at room temperature. The secondary Ab was removed with extensive washing and the parasite DNA was stained for 10 min at room temperature with 10 μg/ml PI (propidium iodide) solution in PBS containing 100 μg/ml RNase. Samples were washed twice with PBS and the coverslips were mounted with Mowiol. Microscopic analysis of the samples was performed by a Leica TCS SP confocal microscope using the 63× apochromat lens.

For quantifying co-localization of *Ld*Ran with LeishH1, the Pearson's correlation coefficient (*r*) and the red/green and green/red pixel correlation, were calculated by the Intensity Correlation Analysis program ImagePro 5 software (Media Cybernetics) from a typical image out of at least 15 cells from three independent experiments.

Cell synchronization and flow cytometry

L. donovani parasites in the exponential phase (~5×10^6/ml) were synchronized with 5 mM HU (hydroxyurea) in the G_1/S-phase border of the cell cycle, as described previously [21]. PI labelling and flow cytometry (FACS) analysis in a FACSCalibur flow cytometer (Becton-Dickinson Immunocytometer System) were performed as described previously [21].

*Ld*Ran and GST–LeishH1 pull-down assays

*Ld*Ran was purified under denaturing conditions (6 M urea), as described above, and maintained bound to the Ni-NTA beads (~2 μg of *Ld*Ran per reaction). The urea was removed by washing the beads five times with 10 bed volumes of PBS (pH 8). The beads were finally resuspended in 1 ml of leishmanial protein extract (2 mg/ml) in PBS (pH 8), containing 5 mM $MgCl_2$, 1 mM PMSF, 2.5 μg/ml aprotinin and 1 μg/ml pepstatin. As a control, 2 μg of GST or GST–Rab1a was immobilized on glutathione–Sepharose 4B beads (GE Healthcare) and incubated with 1 ml of parasite protein extract (2 mg/ml). The binding reaction was performed at room temperature for 3 h. Subsequently, unbound proteins were removed by centrifugation at 1000 ***g*** for 5 min and the beads were washed four times with 10 volumes of PBS (pH 8). Finally, proteins bound to the beads were eluted with an equal volume of elution buffer (50 mM sodium phosphate buffer, pH 8, 300 mM NaCl and 250 mM imidazole) three times.

For the GST–LeishH1 pull-down assays, 2 μg of GST and GST–LeishH1 [21] were immobilized on 50 μl of glutathione–Sepharose 4B beads according to the manufacturer's instructions and incubated for 3 h at room temperature with 1 ml of leishmanial protein extract (2 mg/ml) in PBS containing 5 mM $MgCl_2$, 1 % (v/v) Triton X-100, 1 mM PMSF, 2.5 μg/ml aprotinin and 1 μg/ml pepstatin. Glutathione–Sepharose beads were subsequently washed four times with 20 volumes of PBS containing 5 mM $MgCl_2$ and 1 % (v/v) Triton X-100 and then frozen at −20 °C before their analysis by SDS/PAGE and Western blotting.

RESULTS

Identification and characterization of *Ld*Ran; *Ld*Ran is developmentally regulated

An ORF (open reading frame) encoding a putative leishmanial Ran orthologue was identified (LinJ25.1470) as a single locus on chromosome 25, in the *L. infantum* genome after a search in the *Leishmania* GeneDB database. Primers based on the *L. infantum* LinJ25.1470 ORF were designed and the putative *Ld*Ran gene was amplified and cloned in the bacterial expression plasmid pTriex with a C-terminal His_6 tag.

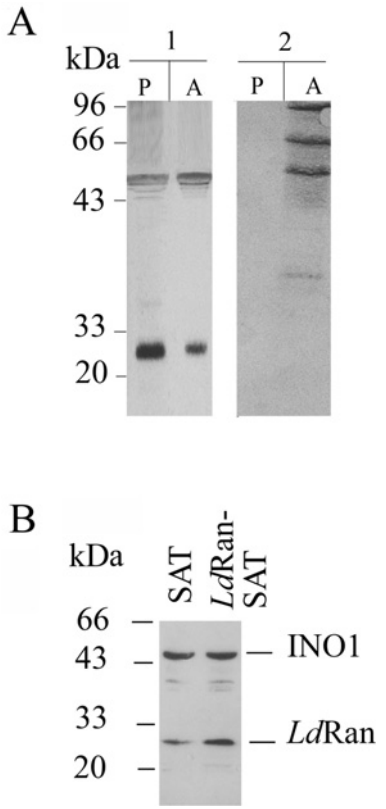

Figure 1 Expression of *Ld*Ran in promastigotes and axenic amastigotes and overexpression of *Ld*Ran in *Ld*Ran-SAT-transfected *L. donovani* parasites

(**A**) *Leishmania* extracts from promastigotes (P) and axenic amastigotes (A) were analysed by SDS/PAGE and subsequently by Western blotting. Total cell extracts from 10^7 promastigotes or amastigotes were loaded per lane. Panel 1: detection of *Ld*Ran protein expression in promastigotes and axenic amastigotes using the anti-*Ld*Ran pAb and an anti-*Lin*INO1 Ab as a loading control; panel 2: detection of A2 protein expression in axenic amastigotes using the anti-A2 C9 mAb. (**B**) Immunoblot analysis of 10^7 *L. donovani* parasites in the stationary phase transfected with either the *Ld*Ran-SAT expression plasmid or with the control plasmid (SAT). To detect *Ld*Ran, anti-*Ld*Ran Ab was used (*Ld*Ran). An anti-*Lin*INO1 Ab (INO1) was used to confirm that equal amounts of parasite extracts were loaded in both lanes. The experiment was performed at least three times. The intensities of the bands were analysed using Alphalmager Software. The fold overexpression was calculated by dividing the band intensity of *Ld*Ran with the band intensity of INO1 and comparing this ratio in *Ld*RanSAT-transfected parasites over the same ratio in control SAT parasites. Molecular masses are indicated in kDa.

The putative *Ld*Ran protein (GenBank® accession number EU426549), was identical with the *Lin*Ran (*L. infantum* Ran) and *Lmj*Ran orthologues. Amino acid sequence alignment of *Ld*Ran with Ran proteins from different species showed that it is highly conserved, having 80 % amino acid sequence identity with Ran orthologues from species as distant as *Homo sapiens*. Western blot analysis using the generated anti-*Ld*Ran Ab showed that *Ld*Ran is expressed in *L. donovani* promastigotes as a ~25 kDa protein, in agreement with the predicted molecular mass (24223 Da) (Figure 1A).

*Ld*Ran expression was also evaluated in axenic amastigotes [21] by Western blot analysis using the *Ld*Ran-specific Ab (Figure 1A) and by immunofluorescence (results not shown). Scanning densitometry of the detected bands revealed that the *Ld*Ran expression level was 3-fold lower in amastigotes. As a

Table 1 Cell-cycle distribution after HU withdrawal in *L. donovani Ld*Ran-SAT and SAT transfectants

Values are from one representative experiment performed four times. All four experiments showed a consistent 8–12 % difference between the control SAT parasite population and the *Ld*Ran-SAT population found in the S- and G_2/M-phases 6 and 10 h after HU release.* $P < 0.05$ compared with corresponding control values (SAT), using a two-tailed paired Student's *t* test.

	Proportion of SAT parasite population (%)			Proportion of *Ld*Ran-SAT parasite population (%)		
Population	G_0/G_1	S	G_2/M	G_0/G_1	S	G_2/M
HU-synchronized	72	11	16	71	9	19
4 h	27	45	28	35	43	22
6 h	19	31	50	25	41*	33*
10 h	39	18	49	34	30*	35*

control for loading an equal number of cells, the blot was probed with *Lin*INO1 antiserum, a 46 kDa protein which is equally expressed in promastigotes and amastigotes [26] (Figure 1A, panel 1). Expression of A2 proteins was also checked with the anti-A2 C9 mAb to ensure that axenic amastigotes had properly differentiated and expressed amastigote-specific proteins as expected (Figure 1A, panel 2).

Overexpression of *Ld*Ran delays cell-cycle progression in *Leishmania*

*Ld*Ran was overexpressed by stable transfection of *L. donovani* parasites with an episomal plasmid. Parasites were viable with no apparent morphological differences from control parasites (bearing plasmid alone, SAT). Overexpression of *Ld*Ran, in the *Ld*Ran-SAT parasites compared with control parasites, was assessed by Western blot analysis and quantification by densitometry which showed a 3-fold (Figure 1B) overexpression. Equal loading was confirmed with the use of an anti-INO1 Ab as a loading control (Figure 1B).

The growth curve of these promastigotes indicated a mild but consistent delay in the exponential phase of their growth (see Supplementary Figure S1A at http://www.BiochemJ.org/bj/424/bj4240367add.htm), suggesting that *Ld*Ran overexpression delays cell division. This effect was more pronounced upon host-free differentiation conditions (see Supplementary Figure S1B). Annexin V–PI staining showed that there was no significant difference in early apoptotic and necrotic (or late apoptotic) control and *Ld*Ran-overexpressing parasites (results not shown). This confirms that the effect is solely due to a delay in growth and not due to increased cell death.

To determine which phase of the cell cycle is affected by *Ld*Ran overexpression we evaluated, using flow cytometry, the cell-cycle progression of *L. donovani* promastigotes overexpressing *Ld*Ran (*Ld*Ran-SAT) and compared it with cell-cycle profiles of control parasites (SAT). SAT and *Ld*Ran-SAT *L. donovani* exponential-phase parasites were synchronized in the G_1/S-phase of the cell cycle with HU (Figure 2 and Table 1). Both SAT and *Ld*Ran-SAT HU-synchronized parasites had a greater percentage of cells in the G_0/G_1-phase of the cell cycle (72 and 71 % respectively) compared with the G_0/G_1-phase of the same asynchronous exponential-phase parasites (55 and 52 % respectively), as expected. At 4 h after release, more parasites overexpressing *Ld*Ran were in the G_1/S-phase border (35 %) compared with control parasites (27 %, Figure 2 and Table 1). At 6 h after release, 31 and 50 % of control parasites were in the S- and G_2/M-phases of the cell cycle, whereas 41 and

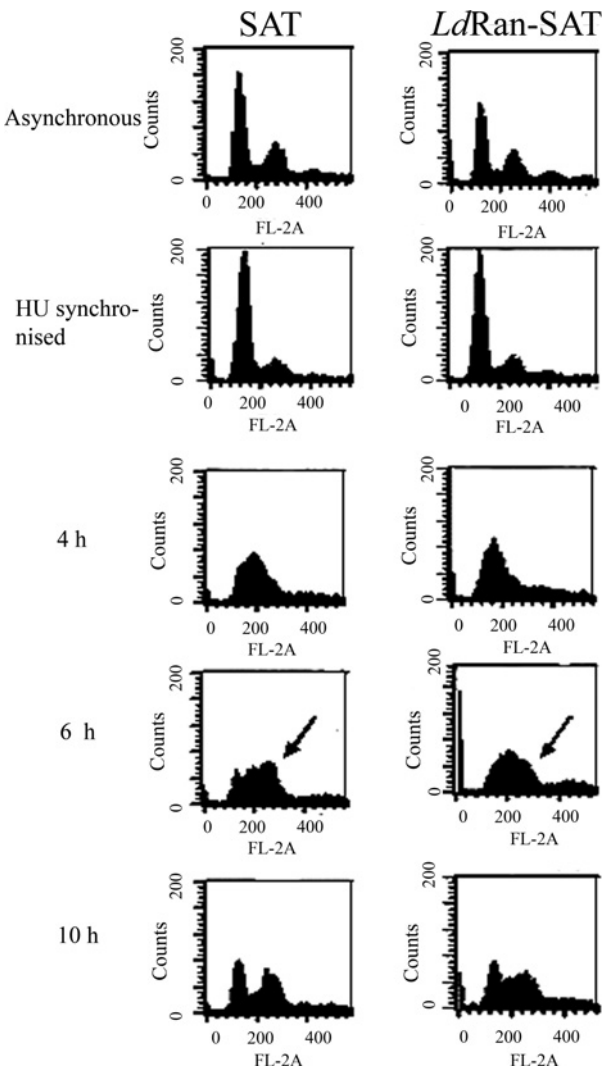

Figure 2 Cell-cycle analysis after HU withdrawal in *Ld*Ran-SAT or SAT *L. donovani* transfectants synchronized at the G_1/S-phase border

The DNA content of control parasites bearing plasmid alone (SAT) or overexpressing *Ld*Ran (*Ld*Ran-SAT) was analysed by flow cytometry in cells stained with PI. The cell-cycle distribution in these cells was calculated using ModFit software. Parasites synchronized with HU at the G_1/S-phase border are indicated as HU-synchronized, 0 h. The time points after release of the HU block are indicated on the left. Not synchronized, exponentially growing parasites are also indicated at the top (asynchronous). Arrowheads at 6 h show the proportion of parasites with 4N (tetraploid) DNA content (G_2/M-phase). The percentage of this population is less in parasites overexpressing *Ld*Ran. A representative experiment of four independently performed experiments is shown.

33 % of *Ld*Ran-overexpressing parasites were in the S- and G_2/M-phases respectively (Figure 2 and Table 1). Therefore *Ld*Ran-overexpressing parasites show a delay in the completion of S-phase. At 10 h after release, there was still a greater percentage of *Ld*Ran-overexpressing parasites in the S-phase, compared with control (30 and 18 % respectively), confirming that *Ld*Ran overexpression causes a constant deregulation of S-phase progression (confirmed in all experiments). This delay in the phases of the cell cycle was calculated to be approx. 2 h with respect to the control parasites, a duration that is significant at the promastigote stage, where the parasite completes one cell cycle within 8–10 h.

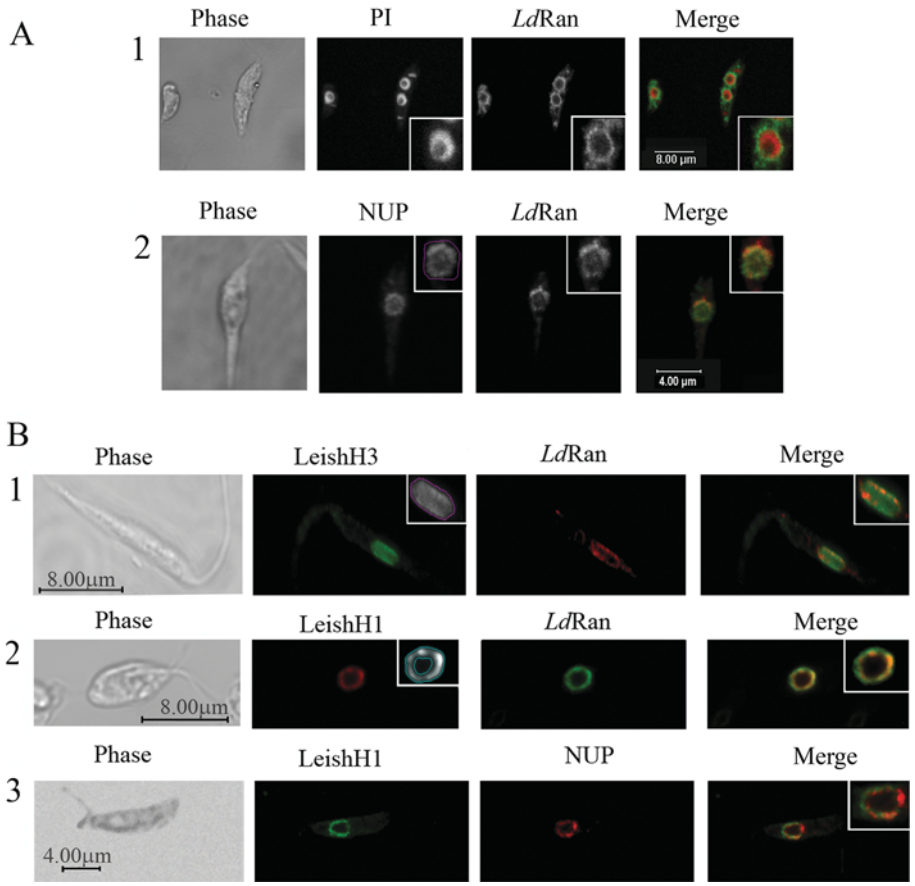

Figure 3 Localization of *Ld*Ran in *L. donovani* promastigotes with respect to LeishH1 and LeishH3

(**A**) Nuclear rim localization of *Ld*Ran in *L. donovani* promastigotes. Row 1: Phase-contrast (Phase) and fluorescence microscopy images in black and white show nuclear and kinetoplast DNA staining with PI and *Ld*Ran staining using a primary anti-*Ld*Ran Ab and a secondary Alexa Fluor® 488-conjugated anti-rabbit Ab. A 2-fold magnification of the nucleus is also shown at the bottom right corner of each image. Merged images of the red (PI) and green fluorescence are shown on the right. Row 2: co-localization of endogenous *Ld*Ran with nucleoporins. Wild-type *L. donovani* promastigotes were stained for nucleoporins (NUP), with an anti-nucleoporin mAb and an Alexa Fluor® 488-conjugated anti-mouse secondary Ab, and for *Ld*Ran (*Ld*Ran) with the rabbit anti-*Ld*Ran pAb and an Alexa Fluor® 546-conjugated anti-rabbit secondary Ab. Fluorescence images are shown in black and white. The parasites analysed are shown in the phase-contrast image on the left (phase), whereas the merged images of the *Ld*Ran (red) and NUP (green) staining are shown on the right. A typical ROI (region of interest) used for quantification of NUP and *Ld*Ran co-localization is shown on the upper right corner of the green channel. A 1.5-fold magnification of the nucleus is shown in the insets of each image. (**B**) *Ld*Ran localization with respect to LeishH1 and LeishH3. Row 1: wild-type *L. donovani* promastigotes were stained for LeishH3 with mouse anti-LeishH3 pAb and an Alexa Fluor® 488-conjugated anti-mouse Ab, and for *Ld*Ran with a rabbit anti-*Ld*Ran pAb and an Alexa Fluor® 546-conjugated anti-rabbit Ab. The average Pearson's correlation coefficient for the *Ld*Ran and LeishH3 intranuclear localization was 0.65 and was calculated from 15 cells from three independent experiments. The average red in green co-localization (*Ld*Ran in LeishH3) was equal to 60 %, whereas the green in red (LeishH3 in *Ld*Ran) was 40 %. Typical ROIs are shown on the upper right corner of the green channel. Row 2: wild-type *L. donovani* promastigotes were stained for *Ld*Ran, with a mouse anti-*Ld*Ran pAb and an Alexa Fluor® 546-conjugated anti-mouse secondary Ab, and for LeishH1 with the rabbit anti-LeishH1 pAb and an Alexa Fluor® 488-conjugated anti-rabbit secondary Ab. The merged images of the LeishH1 (green) and *Ld*Ran (red) staining are shown on the right. The average Pearson's correlation coefficient for the *Ld*Ran and LeishH1 intranuclear localization was 0.9 and was calculated from 15 cells from three independent experiments. The average red in green co-localization (*Ld*Ran in LeishH1) was equal to 90 %, whereas the green in red (LeishH1 in *Ld*Ran) was 80 %. Typical ROIs are shown on the upper right corner of the red channel. Row 3: wild-type *L. donovani* promastigotes were stained for NUP, with an anti-nucleoporin mAb and an Alexa Fluor® 546-conjugated anti-mouse secondary Ab, and for LeishH1 (LeishH1) with the rabbit anti-LeishH1 pAb and an Alexa Fluor® 488-conjugated anti-rabbit secondary Ab. The merged images of the LeishH1 (green) and NUP (red) staining are shown on the right. The parasites analysed for all rows are shown in the phase-contrast images on the left (Phase).

*Ld*Ran at the nuclear envelope co-localizes with linker histone H1

The localization of endogenous Ran in wild-type *L. donovani* promastigotes was assessed using an affinity-purified anti-*Ld*Ran primary Ab. Double staining with PI (Figure 3A, row 1) or detection of FG (Phe-Gly) nucleoporins (Figure 3A, row 2) showed that *Ld*Ran is localized at the nuclear envelope/rim, as is the case for *Lmj*Ran [16], which, as mentioned above, is identical with *Ld*Ran. Quantititative analysis using the ImagePro software showed that 95 % of *Ld*Ran co-localizes with FG nucleoporins, whereas 70 % of FG nucleoporins co-localizes with *Ld*Ran (Figure 3A, row 2). Expression of *Lmj*Ran as a fusion protein with GFP [16], cloned in the plasmid pTH_6cGFPn vector [27], in *L. donovani* showed that that GFP-*Lmj*Ran is localized at the vicinity of the nuclear envelope (results not shown) confirming thereby the specificity of the generated anti-*Ld*Ran Ab used in immunostaining.

Since *Ld*Ran does not predominantly localize in the nucleoplasm of promastigotes we investigated whether *Ld*Ran associates with histones. First we examined the degree of core histone co-localization with *Ld*Ran. For this study we used histone H3, being one of Ran's binding proteins in mammalian cells. We also investigated *Ld*Ran's co-localization with LeishH1, knowing from previous studies that this histone had a nuclear rim localization at least in the majority of parasites (D. Smirlis and K. Soteriadou, unpublished work). For this purpose a rabbit anti-*Ld*Ran and a mouse anti-LeishH3 or a rabbit anti-LeishH1 pAb and a mouse anti-*Ld*Ran pAb were used in double immunofluorescence staining experiments (Figure 3B, rows 1

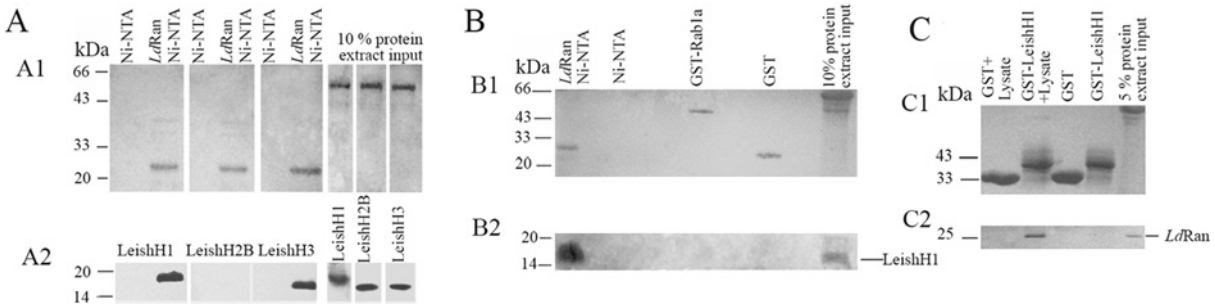

Figure 4 ***Ld*Ran interacts with LeishH1** ***in vitro***

(**A**) Immunoblot analysis of proteins eluted from *Ld*Ran immobilized on Ni-NTA beads using anti-LeishH1, anti-LeishH2B and anti-LeishH3 Abs. Recombinant *Ld*Ran-immobilized Ni-NTA beads (*Ld*Ran Ni-NTA) were incubated with a leishmanial protein extract. An equal volume of Ni-NTA beads (Ni-NTA) was incubated with an equal amount of leishmanial protein extract. Beads were subsequently washed and proteins eluted with imidazole. A 10 % amount of the protein lysate per reaction was also used as a positive control (10 % protein extract input). Panel A1: Ponceau-S staining of the Western blot showing the amounts of *Ld*Ran used per reaction. Panel A2: immunoblot analysis using anti-LeishH1 (LeishH1), anti-LeishH2B (LeishH2B) and anti-LeishH3 (LeishH3) Abs to detect the presence of the corresponding histones. (**B**) GST–Rab1a, GST and *Ld*Ran (2 μg each) were immobilized on glutathione–Sepharose and Ni-NTA beads and incubated with leishmanial protein extract (2 mg). An equal volume of Ni-NTA beads (Ni-NTA) incubated with leishmanial protein extract was loaded to check for non-specific protein precipitation. Panel B1: Ponceau-S staining of the Western blot showing the amounts of GST, GST–Rab1a and *Ld*Ran, used per reaction. Panel B2: immunoblot analysis using an anti-LeishH1 Ab to detect the presence of LeishH1. A 10 % amount of the protein lysate was used as a positive control to detect the presence of LeishH1. (**C**) GST–LeishH1 (2 μg) was immobilized on glutathione–Sepharose beads and incubated with leishmanial protein extract (GST–LeishH1+Lysate). GST protein (2 μg) was immobilized on glutathione–Sepharose beads and incubated with an equal amount of protein extract (GST+Lysate). GST–LeishH1 and GST were also loaded (GST–LeishH1 and GST) as negative controls. A 5 % amount of the protein lysate per reaction was also used as a positive control. Panel C1: Ponceau-S staining of the Western blot showing the amounts of GST and GST–LeishH1 used per reaction. Panel C2: immunoblot analysis using an anti-*Ld*Ran Ab to detect the presence of *Ld*Ran. The experiment was performed twice. Molecular masses are indicated in kDa.

and 2 respectively). Figure 3(B), row1 shows that LeishH3 is predominantly localized in the nucleoplasm of the parasite (in 70 % of the cells LeishH3 was nucleoplasmic, and in 30 % of the cells was closer to the nuclear rim), whereas nuclear *Ld*Ran although present in lower concentrations in the nucleoplasm, was predominantly found at the nuclear rim. *Ld*Ran and LeishH3 showed a moderate co-localization. Quantitative analysis using the ImagePro software showed that 40 % of *Ld*Ran co-localized with LeishH3 and 60 % of LeishH3 co-localized with *Ld*Ran. The Pearson correlation co-efficient indicating the strength and direction of a linear relationship between two random variables, was also moderate ($r = 0.65$). On the other hand, Figure 3(B), row 3 shows that LeishH1 is localized near the nuclear periphery and close to the nuclear envelope. This localization of LeishH1 was not uniform, but was detected in the majority of cells. In more detail, in 75 % of parasites LeishH1 localized at the nuclear rim, where the linker histone did not co-localize with the bulk DNA, and in 25 % of the parasites, LeishH1 was nucleoplasmic. *Ld*Ran co-localizes at the nuclear rim, with LeishH1 (Figure 3B, row 2). More specifically, quantitative analysis showed that 90 % of LeishH1 co-localized with *Ld*Ran and 80 % of *Ld*Ran co-localized with LeishH1, with $r = 0.9$. The co-localization of *Ld*Ran with LeishH1 is significant, taking into account the dynamic nature of Ran and histone H1 proteins [28,29]. This co-localization was found to be independent of the fixation method, and shows clearly that linker histone H1 may be a candidate partner of *Ld*Ran.

LdRan interacts *in vitro* with linker histone LeishH1

To investigate a possible interaction of *Ld*Ran with linker histone H1, we performed *Ld*Ran pull-down experiments. We examined in parallel the interaction of *Ld*Ran with LeishH3, expecting that these proteins interact *in vitro* since the mammalian histone H3 globular domain responsible for binding to Ran [11] is well conserved in *Leishmania* [30]. We also assessed the binding of LeishH2B to *Ld*Ran as a negative control, since the mammalian histone H2B is not known to interact directly with Ran, but via RCC1 [10]. As shown in Figure 4(A) *Ld*Ran interacts with LeishH1 and LeishH3, but it does not interact with LeishH2B. The anti-histone Abs detected histones almost equally well in equally loaded protein inputs used for the binding reactions (Figure 4A). LeishH1 bound equally well to *Ld*Ran as to LeishH3 *in vitro*. Additionally, to verify that *Ld*Ran interacted directly with linker LeishH1, we incubated recombinant histone H1 (cleaved with thrombin from the GST moiety) with *Ld*Ran-bound Ni-NTA beads. LeishH1 was detected on the *Ld*Ran–Ni-NTA beads, whereas no LeishH1 was immobilized on an equal volume of Ni-NTA beads (results not shown), supporting the direct interaction between the two proteins.

To examine the specificity of the interaction of *Ld*Ran with LeishH1, we performed a pull-down assay using murine Rab1a, which is 30 % identical and 50 % homologous with *Ld*Ran. Rab1a was used as a GST-fusion protein, and equal amounts of GST, GST–Rab1a and *Ld*Ran were immobilized on glutathione–Sepharose and Ni-NTA beads respectively (Figure 4B, panel B1). LeishH1 was only detected in beads with immobilized *Ld*Ran (Figure 4B, panel B2).

To eliminate the possibility that the *in vitro* interaction of *Ld*Ran with LeishH1 was due to an 'aberrant' refolding of recombinant *Ld*Ran, equal amounts of GST (used as a negative control) and GST–LeishH1 were immobilized on glutathione–Sepharose beads (Figure 4C) and incubated with leishmanial protein extracts. Additionally, equal amounts of GST and GST–LeishH1 that were not incubated with leishmanial extracts were also used as negative controls (Figure 4C). Beads were washed extensively after the completion of the incubation period. Native *Ld*Ran was present only in GST–LeishH1 and not in GST-bound beads (Figure 4C), indicating that *Ld*Ran interacts specifically with LeishH1. Therefore denaturation and refolding of recombinant *Ld*Ran had no effect on the ability of this protein to interact with LeishH1.

DISCUSSION

The aim of the present study was to characterize the Ran orthologue from *L. donovani*, emphasizing its interaction with histones. The 3-fold down-regulation of *Ld*Ran in axenic

amastigotes was in agreement with results from previous studies showing that the mRNA encoding the leishmanial Ran was down-regulated in amastigotes by a factor of 2.3 compared with the promastigote stage [31] and that the *Ld*Ran protein expression level decreased during differentiation [32]. In the amastigote stage, the parasites undergo a number of changes including morphological ones, deregulation of cell-cycle progression and a decrease in the rate of protein synthesis [33]. Therefore down-regulation of expression in the amastigote stage of a protein involved in essential cellular functions such as regulation of cellular division, cell-cycle progression and nucleocytoplasmic traffic is not an unexpected finding. Overexpression of *Ld*Ran significantly affected the division of parasites during differentiation, suggesting that *Ld*Ran down-regulation is required for appropriate promastigote to amastigote differentiation.

L. donovani promastigotes tolerated overexpression of *Ld*Ran, but these parasites also had a growth defect, linked with the delay in S-phase progression. In mammalian cells, expression of mutants stabilizing Ran in its GTP-bound form [34] or depletion of RCC1 [35] (which results in the enrichment of the GDP-bound form of Ran) both cause a delay in cell-cycle progression, indicating that any disturbance in the GTP/GDP-bound state of Ran may bring deregulation in S-phase progression [36]. Importin-β appears to be dispensable for regulating cell-cycle progression [37], but more investigations are required for revealing the precise mechanism by which Ran modulates cell-cycle progression.

*Ld*Ran, like *Lmj*Ran [16], localizes at the nuclear rim where it co-localizes with FG nucleoporins. Interestingly, *Ld*Ran expressed in mammalian cells (COS7), localizes at the nucleoplasm (results not shown) indicating that the nuclear rim localization of *Ld*Ran is due to parasite-specific interacting proteins. Some of these proteins could be proteins in the Ran network, such as NTF-2 and CAS, and present in the leishmanial nuclear envelope [16].

In metazoan cells, Ran interacts in the nucleoplasm with histones and this interaction occurs via two distinct mechanisms: one being a direct interaction of Ran with core histones H3 and H4 [11], and the other being its indirect interaction with the other two core histones H2A and H2B via RCC1 [10]. The nuclear rim predominant localization of *Ld*Ran in *L. donovani* promastigotes raised the question of whether an *Ld*Ran–histone association occurred. *Ld*Ran as its mammalian counterpart was able to bind to histone H3, but not to histone H2B *in vitro*. Core histones in *Leishmania*, however, are present predominately in the nucleoplasm in contrast with the *Ld*Ran localization at the nuclear periphery. Therefore the moderate co-localization of *Ld*Ran with LeishH3 makes their interaction *in vivo* still speculative. In contrast, LeishH1 was present at the nuclear rim in the majority of cells by at least two methods of cell fixation (results not shown). *Ld*Ran and LeishH1 directly interacted *in vitro* and co-localized at the nuclear rim. This is the first evidence to date of a linker histone interacting with Ran. It is not currently known whether this interaction is unique for *Leishmania* spp., or whether it exists in other organisms. It is known that Ran [14] and histone H1 in plants are both present at the nuclear rim, away from the nucleoplasmic histone H3 [38], but their interaction has not been investigated. Plant histone H1 possesses microtubule-organizing activity, forming ring-shaped complexes with tubulin at atypical MTOCs (microtubule-organizing centres) present in the nuclear periphery of plant cells [38,39]. A possible explanation for the interaction of *Ld*Ran with LeishH1 at the nuclear periphery is its involvement in the organization and elongation of microtubules adjacent to the leishmanial nuclear envelope [40].

Interaction of Ran with chromatin in metazoans has an unknown function in interphase cells. In mitotic cells, it is postulated that the Ran–histone association, required for the formation of a Ran-GTP chromosomal gradient, may play an important role during reassembly of the nuclear envelope by increasing the binding of membranes to the chromatin surface [11] and for the formation of the mitotic spindle [9]. In *Leishmania*, the nucleus does not break down during mitosis [40], therefore the requirement of a Ran-GTP chromosomal gradient for the post-mitotic nuclear envelope assembly is clearly not required. It has been reported that, in the closed mitosis of *Aspergillus nidulans*, the nuclear pores open, allowing passive diffusion of proteins [41]. Thus the Ran-GTP chromosomal gradient may be essential, even in organisms performing a closed mitosis. Therefore one cannot exclude the possibility that the Ran–LeishH1 interaction in *Leishmania* is required to keep a form of an atypical chromosomal nuclear rim Ran-GTP gradient in the nuclear rim chromatin. However, the *Ld*Ran–linker histone H1 interaction may modulate pathways other than those documented for the metazoan Ran–core histone association. In *L. donovani*, LeishH1 regulates cell-cycle progression, promastigote to amastigote differentiation and virulence [21]. Interaction of *Ld*Ran with LeishH1 may be important for the regulation of these processes.

Ran appears to be a master regulator and co-ordinator of events that require intimate cross-talk between chromatin and the cytoplasm, for cell-cycle progression and spindle assembly [42]. In *Leishmania*, these events have similarities, but also major differences from other eukaryotes such as metazoans and yeast. Further investigation is therefore required to elucidate these mechanisms and to define the precise mechanism of *Ld*Ran participation in the cell cycle of this parasite, and whether an atypical Ran-GTP chromosomal gradient is achieved. Finally, the atypical Ran network in this parasite may be exploited for anti-leishmanial drug development.

AUTHOR CONTRIBUTION

Despina Smirlis co-ordinated the work and conducted the molecular work, collected and analysed data and prepared the paper; Haralabia Boleti gave advice on light microscopy and critically read the paper before submission; Maria Gaitanou performed the immunofluorescence in mammalian cells, the cloning and purification of the GST–Rab1a protein and critically read the paper before submission; Manuel Soto provided the recombinant core histones for the generation of antibodies and critically read the paper before submission; Ketty Soteriadou funded the work, analysed the data and significantly contributed to the preparation of the paper.

ACKNOWLEDGEMENTS

We thank Professor Greg Matlashewski (McGill University, Montreal, Quebec, Canada) for donating the A2 monoclonal antibody and Dr Lucien Gobu and Dr Patrick Bastien (CNRS/Montpellier University, Montpellier, France) for the pTH$_6$cGFPn-Ran plasmid and COST (European Cooperation in the field of Scientific and Technical Research) Action BM0802. Finally we thank Georgia Konidou for her technical assistance and the production of the anti-*Ld*Ran pAbs.

FUNDING

This work was supported by the Hellenic Pasteur Institute.

REFERENCES

1 Bischoff, F. R. and Ponstingl, H. (1991) Mitotic regulator protein RCC1 is complexed with a nuclear ras-related polypeptide. Proc. Natl. Acad. Sci. U.S.A. **88**, 10830–10834

2 Bischoff, F. R. and Ponstingl, H. (1991) Catalysis of guanine nucleotide exchange on Ran by the mitotic regulator RCC1. Nature **354**, 80–82

3 Bischoff, F. R., Klebe, C., Kretschmer, J., Wittinghofer, A. and Ponstingl, H. (1994) RanGAP1 induces GTPase activity of nuclear Ras-related Ran. Proc. Natl. Acad. Sci. U.S.A. **91**, 2587–2591
4 Moore, M. S. and Blobel, G. (1994) A G protein involved in nucleocytoplasmic transport: the role of Ran. Trends Biochem. Sci. **19**, 211–216
5 Heald, R. and Weis, K. (2000) Spindles get the ran around. Trends Cell Biol. **10**, 1–4
6 Hetzer, M., Bilbao-Cortes, D., Walther, T. C., Gruss, O. J. and Mattaj, I. W. (2000) GTP hydrolysis by Ran is required for nuclear envelope assembly. Mol. Cell **5**, 1013–1024
7 Ren, M., Drivas, G., D'Eustachio, P. and Rush, M. G. (1993) Ran/TC4: a small nuclear GTP-binding protein that regulates DNA synthesis. J. Cell. Biol. **120**, 313–323
8 Arnaoutov, A. and Dasso, M. (2003) The Ran GTPase regulates kinetochore function. Dev. Cell **5**, 99–111
9 Zheng, Y. (2004) G protein control of microtubule assembly. Annu. Rev. Cell Dev. Biol. **20**, 867–894
10 Nemergut, M. E., Mizzen, C. A., Stukenberg, T., Allis, C. D. and Macara, I. G. (2001) Chromatin docking and exchange activity enhancement of RCC1 by histones H2A and H2B. Science **292**, 1540–1543
11 Bilbao-Cortes, D., Hetzer, M., Langst, G., Becker, P. B. and Mattaj, I. W. (2002) Ran binds to chromatin by two distinct mechanisms. Curr. Biol. **12**, 1151–1156
12 Li, H. Y. and Zheng, Y. (2004) Phosphorylation of RCC1 in mitosis is essential for producing a high RanGTP concentration on chromosomes and for spindle assembly in mammalian cells. Genes Dev. **18**, 512–527
13 Caudron, M., Bunt, G., Bastiaens, P. and Karsenti, E. (2005) Spatial coordination of spindle assembly by chromosome-mediated signaling gradients. Science **309**, 1373–1376
14 Ma, L., Hong, Z. and Zhang, Z. (2007) Perinuclear and nuclear envelope localizations of *Arabidopsis* Ran proteins. Plant Cell Rep. **26**, 1373–1382
15 Frankel, M. B. and Knoll, L. J. (2008) Functional analysis of key nuclear trafficking components reveals an atypical Ran network required for parasite pathogenesis. Mol. Microbiol. **70**, 410–420
16 Casanova, M., Portales, P., Blaineau, C., Crobu, L., Bastien, P. and Pages, M. (2008) Inhibition of active nuclear transport is an intrinsic trigger of programmed cell death in trypanosomatids. Cell Death Differ. **15**, 1910–1920
17 World Health Organization (2006) Control of leishmaniasis, World Health Organization, Geneva, http://apps.who.int/gb/ebwha/pdf_files/EB118/B118_4-en.pdf
18 Chang, K.-P. and Dwyer, D. M. (1978) *Leishmania donovani*. Hamster macrophage interactions *in vitro*: cell entry, intracellular survival, and multiplication of amastigotes. J. Exp. Med. **147**, 515–530
19 McConville, M. J. and Handman, E. (2007) The molecular basis of *Leishmania* pathogenesis. Int. J. Parasitol. **37**, 1047–1051
20 Field, M. C., Field, H. and Boothroyd, J. C. (1995) A homologue of the nuclear GTPase ran/TC4 from *Trypanosoma brucei*. Mol. Biochem. Parasitol. **69**, 131–134
21 Smirlis, D., Bisti, S. N., Xingi, E., Konidou, G., Thiakaki, M. and Soteriadou, K. P. (2006) *Leishmania* histone H1 overexpression delays parasite cell-cycle progression, parasite differentiation and reduces *Leishmania* infectivity *in vivo*. Mol. Microbiol. **60**, 1457–1473
22 Xingi, E., Smirlis, D., Myrianthopoulos, V., Magiatis, P., Grant, K. M., Meijer, L., Mikros, E., Skaltsounis, A. L. and Soteriadou, K. (2009) 6-Br-5-methylindirubin-3′oxime (5-Me-6-BIO) targeting the leishmanial glycogen synthase kinase-3 (GSK-3) short form affects cell-cycle progression and induces apoptosis-like death: exploitation of GSK-3 for treating leishmaniasis. Int. J. Parasitol. **39**, 1289–1303
23 Laemmli, U. K. (1970) Cleavage of structural proteins during the assembly of the head of bacteriophage T4. Nature **227**, 680–685
24 Papageorgiou, F. T. and Soteriadou, K. P. (2002) Expression of a novel *Leishmania* gene encoding a histone H1-like protein in *Leishmania major* modulates parasite infectivity *in vitro*. Infect. Immun. **70**, 6976–6986
25 Iborra, S., Soto, M., Carrion, J., Alonso, C. and Requena, J. M. (2004) Vaccination with a plasmid DNA cocktail encoding the nucleosomal histones of *Leishmania* confers protection against murine cutaneous leishmaniosis. Vaccine **22**, 3865–3876
26 Ilg, T. (2002) Generation of *myo*-inositol-auxotrophic *Leishmania mexicana* mutants by targeted replacement of the *myo*-inositol-1-phosphate synthase gene. Mol. Biochem. Parasitol. **120**, 151–156
27 Dubessay, P., Blaineau, C., Bastien, P., Tasse, L., Van Dijk, J., Crobu, L. and Pages, M. (2006) Cell cycle-dependent expression regulation by the proteasome pathway and characterization of the nuclear targeting signal of a *Leishmania major* Kin-13 kinesin. Mol. Microbiol. **59**, 1162–1174
28 Bustin, M., Catez, F. and Lim, J. H. (2005) The dynamics of histone H1 function in chromatin. Mol. Cell **17**, 617–620
29 Li, H. Y., Wirtz, D. and Zheng, Y. (2003) A mechanism of coupling RCC1 mobility to RanGTP production on the chromatin *in vivo*. J. Cell Biol. **160**, 635–644
30 Soto, M., Requena, J. M., Morales, G. and Alonso, C. (1994) The *Leishmania infantum* histone H3 possesses an extremely divergent N-terminal domain. Biochim. Biophys. Acta **1219**, 533–535
31 Leifso, K., Cohen-Freue, G., Dogra, N., Murray, A. and McMaster, W. R. (2007) Genomic and proteomic expression analysis of *Leishmania* promastigote and amastigote life stages: the *Leishmania* genome is constitutively expressed. Mol. Biochem. Parasitol. **152**, 35–46
32 Rosenzweig, D., Smith, D., Opperdoes, F., Stern, S., Olafson, R. W. and Zilberstein, D. (2008) Retooling *Leishmania* metabolism: from sand fly gut to human macrophage. FASEB J. **22**, 590–602
33 Gupta, N., Goyal, N. and Rastogi, A. K. (2001) *In vitro* cultivation and characterization of axenic amastigotes of *Leishmania*. Trends Parasitol. **17**, 150–153
34 Ren, M., Coutavas, E., D'Eustachio, P. and Rush, M. G. (1994) Effects of mutant Ran/TC4 proteins on cell cycle progression. Mol. Cell. Biol. **14**, 4216–4224
35 Dasso, M., Nishitani, H., Kornbluth, S., Nishimoto, T. and Newport, J. W. (1992) RCC1, a regulator of mitosis, is essential for DNA replication. Mol. Cell. Biol. **12**, 3337–3345
36 Moore, J. D. (2001) The Ran-GTPase and cell-cycle control. BioEssays **23**, 77–85
37 Li, H. Y., Cao, K. and Zheng, Y. (2003) Ran in the spindle checkpoint: a new function for a versatile GTPase. Trends Cell Biol. **13**, 553–557
38 Hotta, T., Haraguchi, T. and Mizuno, K. (2007) A novel function of plant histone H1: microtubule nucleation and continuous plus end association. Cell Struct. Funct. **32**, 79–87
39 Nakayama, T., Ishii, T., Hotta, T. and Mizuno, K. (2008) Radial microtubule organization by histone H1 on nuclei of cultured tobacco BY-2 cells. J. Biol. Chem. **283**, 16632–16640
40 Triemer, R. E., Fritrz, L. M. and Herman, R. (1986) Ultrastructural features of mitosis in *Leishmania adleri*. Protoplasma **134**, 134–162
41 De Souza, C. P. and Osmani, S. A. (2007) Mitosis, not just open or closed. Eukaryotic Cell **6**, 1521–1527
42 Clarke, P. R. and Zhang, C. (2008) Spatial and temporal coordination of mitosis by Ran GTPase. Nat. Rev. Mol. Cell. Biol. **9**, 464–477

Received 14 April 2009/13 August 2009; accepted 22 September 2009
Published as BJ Immediate Publication 22 September 2009, doi:10.1042/BJ20090576

Biochem. J. (2009) **424**, 367–374 (Printed in Great Britain) doi:10.1042/BJ20090576

online data

SUPPLEMENTARY ONLINE DATA

Leishmania donovani Ran-GTPase interacts at the nuclear rim with linker histone H1

Despina SMIRLIS*[1], Haralabia BOLETI*†, Maria GAITANOU‡, Manuel SOTO§ and Ketty SOTERIADOU*

*Laboratory of Molecular Parasitology, Department of Microbiology, Hellenic Pasteur Institute, 127 Bas. Sofias Ave., 11521 Athens, Greece, †Light Microscopy Unit, Hellenic Pasteur Institute, 127 Bas. Sofias Ave., 11521 Athens, Greece, ‡Laboratory of Cellular and Molecular Neurobiology, Department of Biochemistry, Hellenic Pasteur Institute, 127 Bas. Sofias Ave., 11521 Athens, Greece, and §Centro de Biología Molecular Severo Ochoa (CSIC-UAM), Departamento de Biología Molecular, Universidad Autónoma de Madrid, 28049 Madrid, Spain

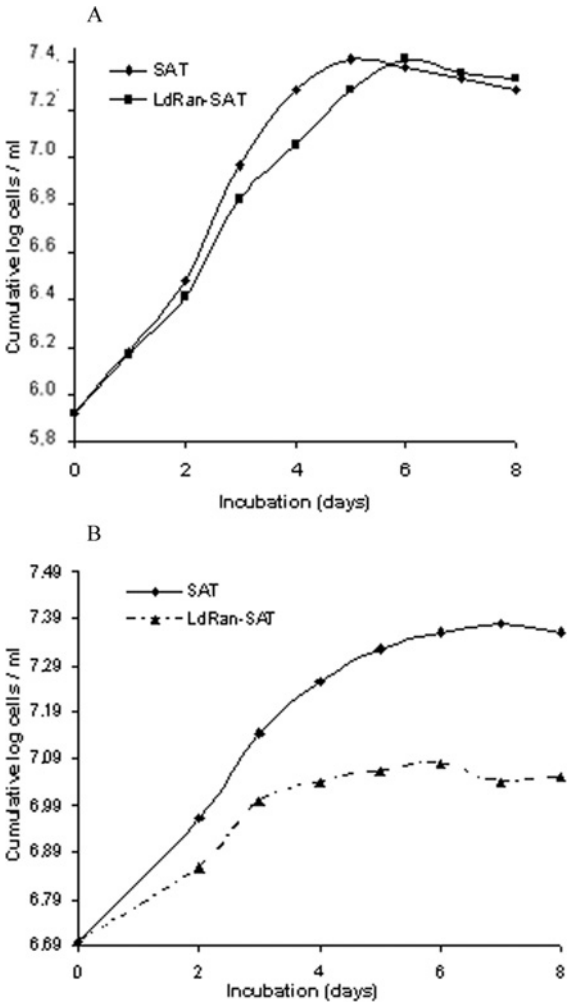

Figure S1 Effect of *Ld*Ran overexpression on parasite growth

Culture growth is shown as cumulative cell numbers during cultivation of *L. donovani* control parasites bearing the plasmid alone (SAT) and parasites overexpressing *Ld*Ran (*Ld*Ran-SAT). Cultures were assayed every 24 h over an 8-day period. (**A**) Effect of *Ld*Ran overexpression on promastigote growth. Results are means for four different experiments, with the S.D. of the actual number of cells not exceeding 20% of the actual value. (**B**) Effect of *Ld*Ran overexpression on parasite growth upon differentiation signal in host-free axenic culture conditions. Parasite numbers are shown as cumulative cell numbers at time points after the differentiation signal (pH 5.5, at 37°C). Results are means for three different experiments, with the S.D. of the actual number of cells not exceeding 20% of the actual value.

Received 14 April 2009/13 August 2009; accepted 22 September 2009
Published as BJ Immediate Publication 22 September 2009, doi:10.1042/BJ20090576

[1] To whom correspondence should be addressed (email penny@pasteur.gr).